

Computational and Experimental analysis of a Counter-Rotating Wind Turbine system

P. Santhana Kumar¹, A. Abraham², R. Joseph Bensingh³ and S. Ilangovan⁴

¹Central Institute of Plastic Engineering and Technology, Chennai.

²Structural Engineering Research Centre-CSIR, Chennai.

^{3,4}Central Institute of Plastic Engineering and Technology, Chennai.

Received 23 May 2012; revised 20 November 2012; accepted 19 February 2013

Wind power is a sustainable and clean source of energy. Single rotor wind turbines (SRWT) of horizontal in nature are the conventional wind turbines, which are used to extract the power from wind. In the past two decades, research have been carried out on Counter Rotating Wind Turbine (CRWT) system and reported that the power extracted is relatively more for a given swept area than that of a SRWT. In the present study, a CRWT, having primary (upwind) and secondary (downwind) rotors with different diameters, which has been reported in a literature is considered and analyzed for its turbine characteristics (power, torque) using commercial software Fluent 6.2 and wind tunnel testing. The flow around the SRWT and CRWT was simulated by using finite volume method coupled with Moving Reference Frame (MRF) technique to solve the governing equations. In this present study the Standard $k-\omega$ shear stress transport turbulence model was considered. For pressure-velocity coupling of the flow second-order upwind discretization scheme (SIMPLEC) was adopted. The results on the power output from SRWT and CRWT using Computational Fluid Dynamics (CFD) have been compared with the literature values. A parametric study on axial distance between two rotors have also been investigated by CFD and it is observed that for 0.65d (d is diameter of primary rotor) the power increase is about 10% for a wind velocity of 10 m/s. Further, a scaled model of CRWT is fabricated using Rapid Prototyping-FDM technique for optimum axial distance of 0.65d with the accuracy of 0.1mm and wind tunnel testing was done with the prony brake-strain gauge assembly for various velocities and it is predicted that there is a power increase for CRWT comparing SRWT.

Keywords: Computational Fluid Dynamics, Single Rotor Wind Turbine, Counter-Rotating Wind Turbine, Power Output, Torque, Axial Distance.

Introduction

Wind power is a significant clean source of renewable energy, and its conversion to usable energy is important, considering the usage/decline of fossil energy sources of earth, it can be utilized effectively for generating the electrical power. In order to obtain energy from wind, more number of wind turbines is being installed¹⁻³. However, regions having high wind energy density are finite⁴. Therefore, research is being conducted to optimize the behavior of wind electric generator units. Some researchers concentrated mainly on the simulation of the performance of the horizontal wind turbine of single rotors using commercial software. Others made comparison between theoretical and experimental studies in the field. Generally, SRWT are used for conventional wind power production systems. A CRWT is described as a system consisting of two rotors separated by an appropriate distance between

them axially. The primary rotor is characterized by a counter-clockwise rotation in upwind location, while the secondary rotor is characterized by a clockwise rotation in downwind location to extract the available energy in the wake efficiently. According to Betz theory⁵, the maximum energy conversion efficiency of conventional wind turbines having a single rotor is about 59%. It is reported that the maximum efficiency obtained by counter rotors having the same swept area is increased to 64%. In the present study, comparison between CRWT with SRWT is made using CFD on power output, 'kW', thrust, 'N' and torque, 'N-m' for each rotor configurations for upwind & downwind location, and the aerodynamic improvement of a CRWT is reported.

Literature Review

In order to increase the power efficiency of wind turbines on CRWT research have been carried out by many investigation⁶⁻²³ and also comparison of power output in CRWT with that of SRWT was reported. Jung *et al.*⁶ has obtained power curve experimentally

*Author for correspondence:
E-mail: kumarpsk@yahoo.co.in

and numerically for a 30 kW CRWT system and also the effects of distance and diameter ratio between two rotors by using Blade Element Momentum (BEM) theory. Appa Energy Systems⁷ has measured the rotor performance and numerical predictions using BEM theory for a prototype of 6 kW CRWT. Shen *et al.*⁸ has predicted the performance of a CRWT having two 500 kW rotors using CFD code (EllipSys3D). Priyono *et al.*⁹ has designed, optimized and studied the characteristics of an Intelligent Wind Turbine using CFD. S.Lee *et al.*¹⁰ investigated the effects of design parameters such as pitch angles, rotating speeds and rotors radius on the aerodynamic performance of a counter-rotating wind turbine and also compared¹¹ aerodynamic characteristics for three kinds of rotor configurations using vortex lattice method. Gupta *et al.*¹² analyzed the performance of a twisted three-bladed H-Darrieus rotor using moving mesh technique in FLUENT 6.2 and also validated the aerodynamic coefficients evaluated by CFD with experimental results. Debnath *et al.*¹³ predicted the performance characteristics for combined three-bucket Savonius and three-bladed Darrieus rotor for various overlap conditions. Mukherji *et al.*¹⁴ performed computational fluid dynamics study on hydrodynamic performance of horizontal axis hydrokinetic turbines and also studied on the velocity distribution, tip speed ratio and power coefficient. John O. Dabiri.¹⁵ performed full-scale field tests for Vertical Axis Wind Turbines in various counter-rotating configurations and achieved higher power output than existing wind turbines. The above mentioned studies have done various researches on wind turbines and also compared the performance of a CRWT with the conventional wind turbines⁶⁻²³.

Principle of CFD Method

The physical aspects of any fluid flow are governed by three principles viz. i) Mass is conserved ii) Newton's second law of momentum (Force = mass \times acceleration) and iii) Energy is conserved. These fundamental physical principles can be expressed in terms of basic mathematical equations, which in their most general form are either integral equations or partial differential equations. Computational Fluid Dynamics is the art of replacing the integrals or the partial derivatives (as the case may be) in equations with discretized algebraic forms, which in turn are solved to obtain numbers for the flow field values at discrete points in time and/or space. The end product of CFD is indeed a collection

of numbers, in contrast to a closed-form analytical solution. However, in the long run, the objective of most engineering analyses, closed form or otherwise, is a quantitative description of the parameters. The mathematical equations describing the aerodynamics of wind turbines²⁴ are based on the equations of conservation of mass and momentum together with other additional equations for the turbulence. In the present study, the Standard k- ω turbulence model is used. The equations for the turbulent kinetic energy, 'k' and the dissipation rate of the turbulent kinetic energy, ' ω ' are solved

Present study

Selection of Blade configuration

In order to predict the performance of a CRWT, initially primary rotor is modeled with appropriate NACA Series aerofoil and following that the secondary rotor is modeled as per the specification, as given in Table 1 with appropriate axial distance between two rotors and diameter ratio (i.e., primary/secondary rotor). The CAD model contains the full geometry of the CRWT system which consists of hub, the primary and secondary rotor. The blade geometry itself is based on a set of 2D-profiles of NACA-0012, NACA-4415, for both the rotors that enabled to give aerodynamic representation of the relevant structure. The 3D model with the constraints is generated using CAD software. The primary rotor and secondary rotor are developed with the given specification of constant diameter ratio (1:2) and optimized axial distance (0.25d to 0.75d) with built in twist (-2°) for NACA-0012 and NACA-4415 aerofoil coordinates to a scale of 1:1.

Computational Analysis

The developed model of CRWT using CATIA software has been imported to CFD domain. The equation of fluid flow is usually solved in Stationary (or inertial) Reference Frames (SRF). However, there are many fluid flow problems that require the equations to be solved in Moving (or non-inertial)

Table1—Specifications of a CRWT System⁶

Specifications	Primary Rotor	Secondary Rotor
No. of blades	3	3
Rotor diameter	5.5 m	11 m
Rotor position	Upwind	Downwind
Airfoil	NACA 4415	NACA 0012
Rotation	Clockwise	CounterClockwie
Built-in twist ($^\circ$)	0°	-2°

Reference Frames (MRF). The computational domain is extended in axial direction (x) for a distance of $2d$ from the secondary rotor in the upstream direction and for a distance of $5d$ from the secondary rotor in the downstream direction, where d is primary rotor diameter (Fig. 1). In the vertical direction (y), the cylindrical domain is extended for a distance of $2.5d$ from the centre of secondary rotor. The computational domain is meshed with Tetrahedral elements of 1112000 numbers. The domain enclosing CRWT system is meshed with triangle face elements due to the varying aerodynamic properties in this region. After the mesh generation, the appropriate flow boundary conditions are specified and explained as follows: (a) Wall (no-slip) boundary conditions are used for the blade surfaces for primary and secondary rotor; (b) Inlet condition: This boundary condition is to specify the air flow velocity (2m/s - 14m/s) with the turbulence intensity of 0.2% ; (c) Outlet condition: This boundary condition is to specify the pressure (Pa); (d) Symmetry boundary conditions are used for the outer cylinder of the cylindrical region representing the limit of the computational domain and (e) Interior boundary condition is used for the interior part of primary rotor and secondary rotor for the usage of MRF.

For the iteration process in numerical method, the Standard $k-\omega$ shear stress transport turbulence model was considered with MRF technique and the second order upwind method was adopted for pressure-velocity coupling of the flow. The convergence criteria for the continuity, momentum, turbulent kinetic energy and RANS were set to 0.01 .

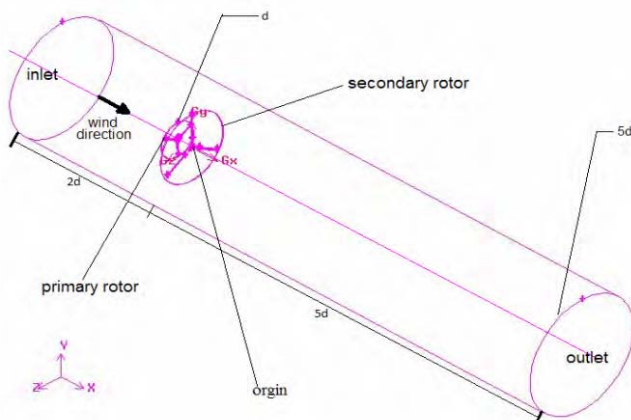


Fig.1—Computational domain of CRWT.

Wind Tunnel Experimental Analysis

The minimum turbulence level Boundary Layer Wind Tunnel at SERC wind laboratory was used in the experimental work. The tunnel is an open circuit blower type of test section 18m long, 2.5m wide and 1.8m height with velocity up to 55m/s . Counter Rotating Wind Turbine (CRWT) with the primary rotor and secondary rotor is fabricated from ABS (Acrylonitrile butadiene styrene) Material with the specification on Table.1.with the scale ratio of $1:20$ is done by $Nd/v = \text{constant}$ (Scaling between real and model system, where N -Rotor Rpm, d -Rotor Diameter, v -velocity). NACA 4415, NACA 0012 profile was used from the blade root to tip with the specified twist and chord distribution for the primary rotor and secondary rotor respectively. The CRWT with the hub and tower assembly is fabricated with the RAPID PROTOTYPING-Fused Deposition Modeling Technique with the layered contour cad data available from the .STL file with the accuracy of 0.1mm is shown in Fig. 2. The CRWT blades were attached to the hub in the horizontal shaft. The primary rotor shaft and secondary rotor shaft is mounted on the support arm with each shaft holding a low friction roller bearing to ensure CRWT shaft rotational freedom. The CRWT shaft assembly with the support arm was mounted on a vertical tower of height of 500mm (L = Diameter of the secondary rotor) and a prony brake assembly with strain gauge setup was located in the both the shafts to measure the torque of the primary and secondary rotor. A digital laser tachometer of accuracy 0.02% was used with reflecting sticker in the hub/blades to measure the rotational speed of the both the rotors. The wind tunnel test section mean velocity was measured



Fig. 2—Experimental setup of CRWT model with prony brake assembly

using hot wire anemometer/Pitot-tube manometer. The tunnel was calibrated for different fan rpm with corresponding test section velocities. The prony brake assembly was calibrated with strain gauge arrangement for different weights from 5 gm to 200 gm. The experimental setup with the prony brake assembly for measurements in the wind tunnel is shown in Fig. 2. The ratio of model area to wind tunnel test section area was less than 5% justifying the neglect of blockage effects.

The torque obtained from the primary rotor and secondary rotor are calculated from the frictional force which is equal to the difference in the strain gauge (or) spring balance while the rotor is in optimum tip speed ratio and rotation rpm. The power of the CRWT is given by $P = 2\pi NT/60$ where, N-Rotor RPM and T-Torque in N-m. The calibration of Strain gauge with the prony brake assembly is done with the various weights from 0 gm to 200 gm after zero balancing of the strain gauge. Wind tunnel testing was done for CRWT model with the axial distance of 0.65d for wind speeds from 3 to 5m/s.

CFD Results and Discussion

Parametric investigation on axial distance between rotors

It is reported in the literature [6] that the maximum power increase by about 20% was obtained when the size of primary rotor is 0.5 times of secondary rotor, when compared with SRWT. In the present study, for the same diameter ratio (1:2) numerical simulation was carried out for various axial distances between two rotors in order to find the appropriate axial

distance, which may give increased power. Hence, a parametric investigation have been carried out for the axial distance of 0.25d, 0.50d, 0.65d and 0.75d (d is the primary rotor diameter) as against 0.125d, 0.25d, 0.375d and 0.50d, as reported in the literature. The effect of axial distance between two rotors on the increase of power (%) has been studied and compared, as shown in Fig. 3(a). It is observed that the power increase of 8.9% at an axial distance of 0.50d for a wind speed of 10 m/s predicted by CFD agrees well with the literature [6] value. Further, it is observed that the maximum power increase by about 9.67% at an axial distance of 0.65d for a wind speed of 10 m/s. Beyond 0.65d, the power increase of CRWT is reduced to 7.8% at an axial distance of 0.75d, due to the energy extraction from the wake of the primary rotor.

Since the primary rotor, which has one-half of the secondary rotor diameters, is located upwind of the secondary rotor, the near wake behavior of the primary rotor is important and can be determined prior in the aerodynamic performance prediction of the turbine system. Hence, axial velocities at various x/d ranging from -1 to +1 having 0 as origin (where the secondary rotor being positioned) was carried out. Typical contours of axial velocities distributions obtained at x/d = -0.7, -0.3, -0.1 and +0.1 are shown in Fig. 3(b). It can be seen that the axial velocity before primary/secondary rotor are subjected to decelerated and having sub-zero values near the blade surfaces i.e., at x/d = -0.7 and -0.1, due to backflow effect. At x/d = -0.3, the axial velocities are observed

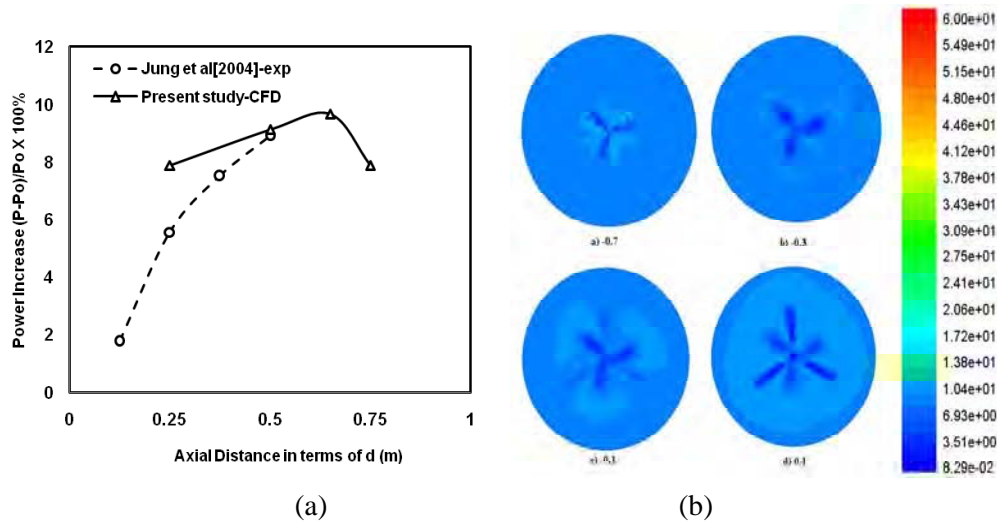


Fig. 3—(a) Comparison of power increase $((P-P_0)/P_0 \times 100\%)$ and (b) Typical contours of axial velocities for various x/d locations for wind speed of 10 m/s [P is the power of the CFD model and P_0 is the power without considering the wake effects]

to be accelerated in the wake of the primary rotor and thus influencing the secondary rotor to extract more energy from the wake of the primary rotor. In this paper, an attempt was made to understand the flow field within stream tube and outside of the stream tube i.e., in the radial direction. A total number of eight different locations ranging from $1/8$ to $10/8$ primary rotor diameter, in which four points are located inside of the stream tube and the other four are located outside of the tube, selected to identify the flow fields around the rotor disk. Fig. 4 shows the complete wind velocity profiles for the above mentioned data points, before and after the primary/secondary rotor at various x/d ranging from -1 to $+1$ and for different y/d ranging from -1.25 to $+1.25$ i.e., in the radial direction as well as the possible boundary of the stream tube. It is observed that at $x/d = -1$, the axial velocity distribution is found to be uniform and when the flow approaches in the longitudinal direction i.e., at $x/d = -0.75$, the axial velocity decelerates within the swept area of the primary rotor in upwind direction and accelerates behind it gradually (i.e., from $x/d = -0.5$ to -0.25), when the flow approaches to the secondary rotor. The phenomenon which is observed in case of primary rotor is observed for the secondary rotor also. It is interesting to note that the distribution of axial velocity within the swept

area of the secondary rotor is getting accelerated when flow approaches beyond $x/d = +1$.

Comparison of power output between SRWT and CRWT

CFD analysis has been carried out on SRWT and CRWT for power output under various wind velocities ranging from 2 m/s to 14 m/s. Comparison on variation of power output for SRWT with literature is shown in Fig. 5. It is observed that the power output (kW), predicted by CFD for the above wind velocities are lower than that of literature values. Comparison on variation of power output for CRWT with the literature is shown in Fig. 5. It is observed that the power output (kW), predicted by CFD for the above wind velocities compares well with that of literature values.

Experimental-Results and Discussion

Evaluation of torque

Experimental work has been carried out for SRWT and CRWT ($0.65d$) on turbine characteristics such as torque (N-m) and power output (Watts) for the scaled model of $1:20$ in the Boundary wind tunnel for wind speed of 3.15 m/s, 3.78 m/s, 5 m/s. The prony brake assembly with the strain gauge is used for the prediction of the torque. Torque (N-m) for various wind speeds is plotted for SRWT and CRWT ($0.65d$) as shown in Fig 6(a). Comparing the two rotor

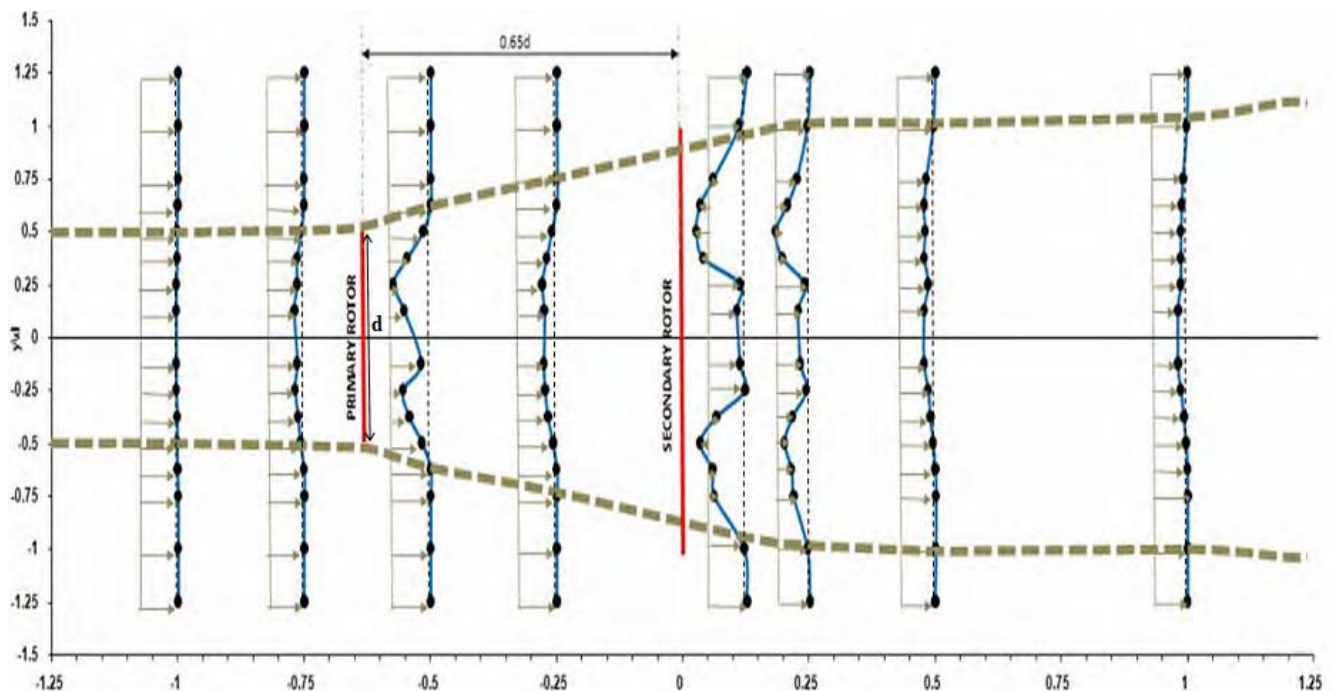


Fig. 4—Velocity profiles along the axial direction

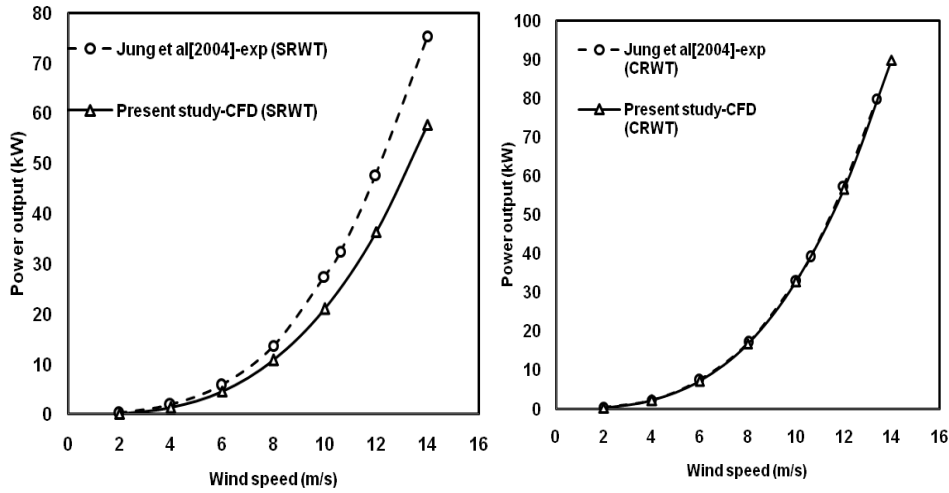


Fig. 5—Comparison of power output for SRWT & CRWT

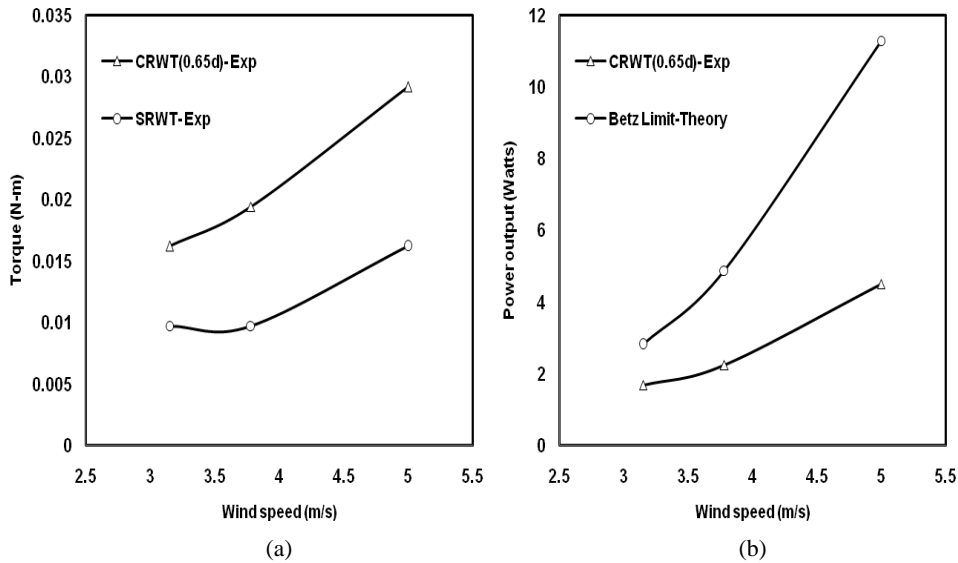


Fig. 6—(a) Variation of torque b) Comparison of power output for CRWT

configurations the torque values of 0.65d axial distance CRWT scaled model produces more than the SRWT. Approximately at 5m/s 0.015 N-m is obtained for SRWT at the same wind speed 0.03N-m is obtained for CRWT due to presence of secondary rotor in the wake.

Comparison of Power Output for CRWT

Experimental work has been carried out on CRWT for power output under various wind speeds. Comparison on power output for CRWT with Betz limit is shown in Fig.6(b). The power of the CRWT model can be calculated from the torque that is

produced by the rotor and its rotational speed. It is observed that the power output (kW) is increased as the wind speed increases which shows the increment in aerodynamic efficiency and also comparing the betz limit (59%) of theoretical power for wind Speeds 3.15 m/s, 3.78 m/s, 5 m/s with the experimental results of the scaled CRWT 0.65d axial distance model it predicts lower and approximately 25-30% of efficiency is produced and this is due to mechanical wear losses in prony brake assembly and also because of wake and tip losses, boundary layer drag, and non ideal flow.

Conclusions

CFD analysis has been carried out on a CRWT having diameter ratio 1:2 with various axial distances of 0.25d, 0.50d, 0.65d and 0.75d. The effect of axial distance between two rotors on the increase of power has been studied and compared with literature. Based on CFD analysis, it is observed that the maximum power increase by about 9.67% at an axial distance of 0.65d for a wind speed of 10 m/s as against the power increase of 8.9% at an axial distance of 0.50d for the same wind speed reported in the literature. Investigation on axial velocity contours for axial distance of 0.65d shows that axial velocity of 8.2 m/s is attained in the wake of the primary rotor at -0.3d location i.e., before the secondary rotor, this makes the secondary rotor to extract more energy from the wake from the primary rotor. Further, experimental work was carried out in boundary wind tunnel in SERC for the scaled CRWT model of 1:20 for various velocities with the prony brake assembly for the torque measurements to ensure the power of the CRWT. When comparing the torque output of the SRWT and CRWT it resembles that CRWT produces more torque at 5m/s comparing other experiments. Theoretical power available for the CRWT with betz limit (59%) was compared with the experimental scaled model CRWT for 0.65d axial distance and its predicts that 25-30% of efficiency from the experimental scaled model and this reduction in power is due to wear in the prony break assembly and also because of wake and tip losses, boundary layer drag, and non ideal flow. Comparing the theoretical power with CFD model 40-50% efficiency is obtained and this increase in CFD model is due to over prediction of numerical simulation without the wake and tip losses.

Acknowledgements

This paper is being published with the kind permission by Director-CSIR-SERC, Chennai & Director General-CIPET. This work has been carried out at WEL-CSIR-SERC, Chennai & ARSTPS-CIPET, Chennai. The support rendered by CSIR-SERC & CIPET is sincerely acknowledged.

References

- Sathyajith Mathew, *Wind Energy Fundamentals, Resource Analysis and Economic* (Springer), 2006, 18.
- Ushiyama I, Small Wind Turbines in Sustainable Urban Environment in *Urban Planning - Sustainable Cities in the framework of the German* (Japan), 2005.
- Lahmeyer International GmbH, Zafarana KfW IV Wind Farm, *Project Design Document (CDM PDD)*, Ver. 03.1, 2008, 1-57.
- IS-875(Part 3-wind loads), *Bureau of Indian Standards*, 1987-reaffirmed 2003, 7-13.
- J.F. Manwell, J.G. McGowan & A.L. Rogers, *Wind Energy Explained, Theory, Design and Application*, (John Wiley & Sons Ltd.,) 2002, 84–88.
- S. Jung, T. No, & K. Ryu, Aerodynamic performance prediction of a 30 kW counters rotating wind turbine system, *Renew Ener*, **30** (2005) 631–644.
- K. Appa, *Energy Innovations Small Grant (EISG) Program (Counter Rotating Wind Turbine System)*, EISG Final Report, (California, US) 2002.
- W.Z. Shen, V.A.K. Zakkam, J.N. Sorensen & K. Appa, Analysis of counter-rotating wind turbines, *J Phys*, (2007) 75.
- Priyono Sutikno & Deny Bayu Saepudin, Design and Blade Optimization of Contra Rotation Double Rotor Wind Turbine in *IJMME-IJENS* **11(1)**, 16-25.
- Seungmin Lee, Hogeon Kim, Eunkuk Son & Soogab Lee, Effects of design parameters on aerodynamic performance of a counter-rotating wind turbine, *Renew Ener*, **42**(2012) 140.
- Seungmin Lee , Hogeon Kim & Soogab Lee, Analysis of aerodynamic characteristics on a counter-rotating wind turbine, *Curr App Phys.*, **10** (2010) S339.
- R. Gupta & Agnimitra Biswas, Computational fluid dynamics analysis of a twisted three-bladed H-Darrieus rotor, *J Renew Sust Ener*, **2** (2010) 043111.
- Biplab Kumar Debnath, Agnimitra Biswas & Rajat Gupta, Computational fluid dynamics analysis of a combined three-bucket Savonius and three-bladed Darrieus rotor at various overlap conditions, *J Renew Sust Ener*, **1** (2009) 033110.
- Suchi Subhra Mukherji, Nitin Kolekar, Arindam Banerjee & Rajiv Mishra, Numerical investigation and evaluation of optimum hydrodynamic performance of a horizontal axis hydrokinetic turbine, *J Renew Sust Ener*, **3** (2011) 063105.
- John O. Dabiri , Potential order-of-magnitude enhancement of wind farm power density via counter-rotating vertical-axis wind turbine arrays, *J Renew Sust Ener*, **3** (2011) 043104.
- Neff D.E. & Meroney R.N., Mean wind and turbulence characteristics due to induction effects near wind turbine rotors, *J Wind Engg and Ind Aerod*, **69–71** (1997) 413–22J.
- J.D. Booker, P.H. Mellor , R. Wrobel & D. Drury, A compact, high efficiency contra-rotating generator suitable for wind turbines in the urban environment, *Renew Ener*, **35** (2010) 2027-2033.
- Hartwanger, David & Horvat.A, 3D Modeling of a wind turbine using CFD in *NAFEMS UK Conf* (Cheltenham, United of Kingdom), 10-11 June 2008.
- Ushiyama, I., Shimota, T. & Miura. Y, An Experimental Study of the Two Staged Wind Turbines in *Proc World Renew Ener Conf*, 1996, 909-912.
- Saravanan P, Paramasivam K M & Selvi Rajan, Pressure distribution of rotating small wind turbine blades with winglet using wind tunnel, *J Sci & Ind Res*, **71** (2012) 425–429.
- S. Chitra Ganapathi, P. Harikrishna, A. Abraham, S. Arunachalam & N. Lakshmanan, Evaluation of force coefficients for a2-dangle section usingrealizable $k-\epsilon$ turbulence model in *SAP Conf on Wind Engg* (Taipei, Taiwan), 8-12 November 2009.
- M. Keerthana & S. Selvi Rajan et al, Numerical studies on evaluation of aerodynamic force coefficients of cable-stayed bridge deck, *J wind & Engg*, **8** (2011) 19-29.
- P. Santhana Kumar, R. Joseph Bensingh & A. Abraham, Computational Analysis of 30KW Contra Rotor Wind Turbine, *ISRN Renew Ener*, (2012) Article ID 939878.
- Jiyauan Tu., *Computational Fluid Dynamics – A Practical Approach* (Elsevier Inc.), 2008, 65